EC Radiation Transport in Fusion Reactor-Grade Tokamaks: Parameterization of Power Loss Density Profile, Non-Thermal Profile Effects under ECCD/ECRH conditions

K.V. Cherepanov 1), A.B. Kukushkin 1), L.K. Kuznetsova 1), E. Westerhof 2)
1) NFI RRC "Kurchatov Institute", Moscow, 123182, Russia
2) FOM-Institute for Plasma Physics Rijnhuizen, Association EURATOM-FOM, Trilateral Euregio Cluster, The Netherlands, www.rijnh.nl

e-mail contact of A.B. Kukushkin: kuka@nfi.kiae.ru

Abstract. Electron cyclotron radiation (ECR) was shown to contribute significantly to the local energy balance in the central part of the plasma column in steady-state scenarios of ITER operation. Strong sensitivity of the net ECR power loss density profile, $P_{EC}(r)$, to the presence of superthermal electrons was shown for ITER scenario 2 (Inductive). Here we report on solving the following three tasks for ITER-like conditions: (1) approximate analytic description of the profile $P_{EC}(r)$ for *maxwellian* plasmas in fusion reactor-grade tokamaks, tested vs. calculations with the code CYNEQ and to be used as a simple simulator during the transport calculations; (2) modeling of deviations of the electron velocity distribution function (EDF) from a maxwellian, caused by the ECCD/ECRH at low harmonics of the cyclotron frequency (O-mode, n=1), using the beam tracing code TORBEAM and the Fokker-Planck code RELAX; (3) modeling, with the code CYNEQ, of the profile $P_{EC}(r)$ for the non-maxwellian EDF of item 2 to evaluate the influence of ECCD/ECRH-produced superthermal electrons on the profile $P_{EC}(r)$, which, for the ITER case, is dominated by the transport of plasma's ECR at harmonics n~3-10. The combined calculations with the codes TORBEAM+RELAX+CYNEQ for scenario 2 predict maximal impact of the ECCD-produced superthermal electrons on the profile $P_{EC}(r)$ (a ~ 20% rise in the core) for oblique launch with full power deposition in the center (e.g., for equatorial launch at 170 GHz, O-mode, n=1, with toroidal injection angle ~ 20°).

1. Introduction

Electron cyclotron radiation (ECR) was shown [1] to contribute significantly to the local energy balance in the central part of the plasma column in steady-state reference scenarios of ITER operation. It becomes the dominant electron cooling mechanism in the center at temperatures exceeding 40 keV. These results were obtained via coupling of the code CYTRAN for ECR transport in maxwellian plasmas with the code ASTRA for tokamak global transport. Strong sensitivity of the net ECR power loss density profile, $P_{EC}(r)$, to the presence of superthermal electrons was shown in [2(A,B)] for ITER scenario 2 (Inductive).

Here we report on solving the following three tasks for ITER-like conditions: (1) approximate analytic description of the profile $P_{EC}(r)$ for *maxwellian* plasmas in fusion reactor-grade tokamaks, (2) modeling, with the codes TORBEAM [3] and RELAX [4], of deviations of the electron velocity distribution function (EDF) from a maxwellian, caused by the ECCD/ECRH at low harmonics of the cyclotron frequency, (3) modeling, with the code CYNEQ [2], of the profile $P_{EC}(r)$ for the non-maxwellian EDF of item 2 to evaluate the influence of ECCD/ECRH-produced superthermal electrons on the profile $P_{EC}(r)$, which, for the ITER case, is dominated by the transport of plasma's ECR at harmonics n~3-10.

The calculations are carried out for the following profiles of plasma density and temperature, taken close to those in the ITER scenario 2 (Inductive), predicted by the ASTRA code 1D simulations [5] (major/minor radius 6.2/2 m, $B_T(0)$=5.3 T):

$$n_e(\rho) = n_e(1) + \left(n_e(0) - n_e(1)\right)\left[1-\rho^2\right]^{0.1}, \quad n_e(0)/n_e(1) = 1/0.5\cdot 10^{20} m^{-3}, \qquad (1)$$

$$T_e(\rho) = T_e(1) + \left(T_e(0) - T_e(1)\right)\left[1 - \rho^2\right]^{1.5}, \quad T_e(0)/T_e(1) = 25/2\ keV. \tag{2}$$

Also, the case of a higher central temperature, namely,

$$T_e(0)/T_e(1) = 35/2\ keV, \tag{3}$$

with the same density profile is considered, as suggested by the calculations [1] for ITER steady-state operation.

2. Analytic Description of ECR Power Loss Density Profile

Transport of the ECR in the fusion reactor-grade tokamaks (high temperature and strong toroidal magnetic field) is such that the radiation emitted in the hot center is strongly absorbed in the relatively cold periphery of the plasma column [6(A),7(A),8]. Under these conditions, the distribution of the net ECR power loss density over magnetic surfaces, $P_{EC}(r)$, appears to be more sensitive to profiles of plasma parameters than total, volume-integrated ECR power loss, P_{EC}^{tot}. In particular, strong local enhancement of the ECR source, caused by superthermal electrons, practically would not change the value of P_{EC}^{tot} in the ITER scenario 2 [2(A,B)].

The necessity to model the operation of reactor-grade tokamaks with fast routine transport codes (cf. [5]) requires parameterization of the profile $P_{EC}(r)$, in addition to parameterization [8] of the ECR total power loss. Here we propose an analytic description tested vs. calculations with the code CYNEQ [2] and to be used as a simple simulator during the transport calculations for ITER-like range of parameters.

The parameterization is based on the further simplification of the well-known fast-routine code CYTRAN [6(B)] with an accent on the satisfactory description of the profile $P_{EC}(r)$ in the core and medium region of the plasma column, i.e. in the range of high enough temperatures, where fitting formulae [6(B)] for spectral dependence of ECR absorption coefficients, averaged over the angles of emitted radiation, in maxwellian plasmas are of good accuracy (~20% for 10 < Te < 120 keV and $\omega/\omega_B > 3$). Note that CYTRAN was proposed for describing $P_{EC}(r)$ in plasmas of the advanced, low-radioactivity fuel-based reactors (D-He^3, D-D, etc.) which require higher burning temperatures and where ECR power loss appears to be the major channel of plasma cooling.

For ITER-like conditions the high harmonics of the fundamental EC frequency dominate in the EC transport. Under these conditions, following the approach of the code CYTRAN, it is possible to reduce the ECR transport problem to a 1D one, in which the profile of the net ECR power loss density depends on the magnetic surface only, and the EC intensity is isotropic and homogeneous in the major part of the reduced phase space {radiation frequency, magnetic surface}, see. Eq. (2) in [7(B)]. This analytic description, which simplifies the respective approximation in [6(B)] via neglecting the diffusion-type contribution of the optically thick core of the plasma column, can be simplified further to give the following result for spectral temperature of EC radiation for extraordinary (X) and ordinary (O) waves (here mixing of the modes due to reflection from the wall is neglected, and the profile of total magnetic field, averaged over magnetic flux surfaces, is taken to be uniform):

$$T_{ECR}(\omega,K) = <T_{cut}(\omega,K)>\left[1 + \frac{(1-R_{WK})}{4\tau n_e(\rho_{cut}(\omega,K))\,\chi_K(\omega,<T_{cut}(\omega,K)>)\,(1-(\rho_{cut}(\omega,K)^2)}\right]^{-1}, \tag{4}$$

where K = X, O; and the fitting formulas [6(B)] for the normalized absorption coefficients χ are slightly modified to avoid the increasing errors at small temperatures:

$$\log_{10}(\omega^2\chi_X(\omega,T_e)) = 1.45 - 7.8\,(\,0.045 + (\omega-2)/T_e\,)^{1/2}, \quad (5)$$

$$\log_{10}(\omega^2\chi_O(\omega,T_e)) = 2.45 - 8.58\,(\,0.18 + (\omega-1)/T_e\,)^{1/2}, \quad (6)$$

ω is radiation frequency in the units of EC fundamental frequency ω_{B0}, T_e is in keV, $\tau = 6\cdot10^3 a/B_0$ is characteristic optical thickness (a, one-dimensional minor radius in meters, B_0, magnetic field in Tesla), R_{WK} is wall reflection coefficient for K mode,

$$<T_{cut}(\omega,K)> = (f\,T_{cut}(\omega,K) + (1-f)\,T_e(1)); \qquad T_{cut}(\omega,K) = T_e(\rho_{cut}(\omega,K)); \quad (7)$$

where $T_e=T_e(\rho)$, $\rho=r/a$, f=0.6; the boundary of optically thick core in the radiation's reduced phase space {frequency, radius} (cf. Eq. (1) in [7(B)]) is described by the relations

$$\omega_{cut}/\omega_{B0} = 2 + D_K\,(1-\rho_{cut}-\rho_{Kmin}), \quad (8)$$

$$D_K = (T_e(0) + T_e(1))/2\ \{\ \ln(\tau n_e(0))/C_K\ \}^2 + A_K, \qquad A_X = 0, \quad A_O = -1, \quad (9)$$

where $\rho_{Kmin} = 0.01$; $C_X = 17.9$; $C_O = 19.7$; and $n_e(0)$ is in 10^{20} m^{-3} units. Also, $\omega_{cut}/\omega_{B0}= 2$ for $\rho > 1-\rho_{Kmin}$, and $\rho_{cut} = 0$ for $\omega/\omega_{B0} > 2 + D_K\,(1-\rho_{Kmin})$.

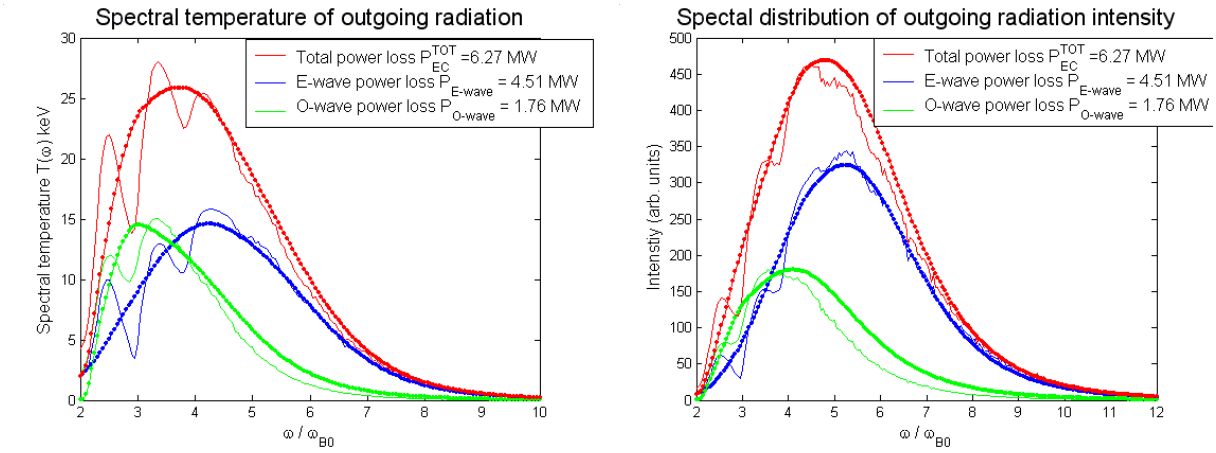

FIG. 1. Spectral distribution of EC radiation temperature (left picture) ($T_{ECR}(\omega)$ in Eq.(4)), and of intensity of outgoing radiation ($\propto \omega^2 T_{ECR}(\omega)$) (right), for the profiles of Eqs. 1,2 and wall reflection coefficient R_{WK}=0.6. Solid – CYNEQ calculations, dots – Eq. (4). Blue, green and red curves correspond to, respectively, X and O modes, and the sum of modes.

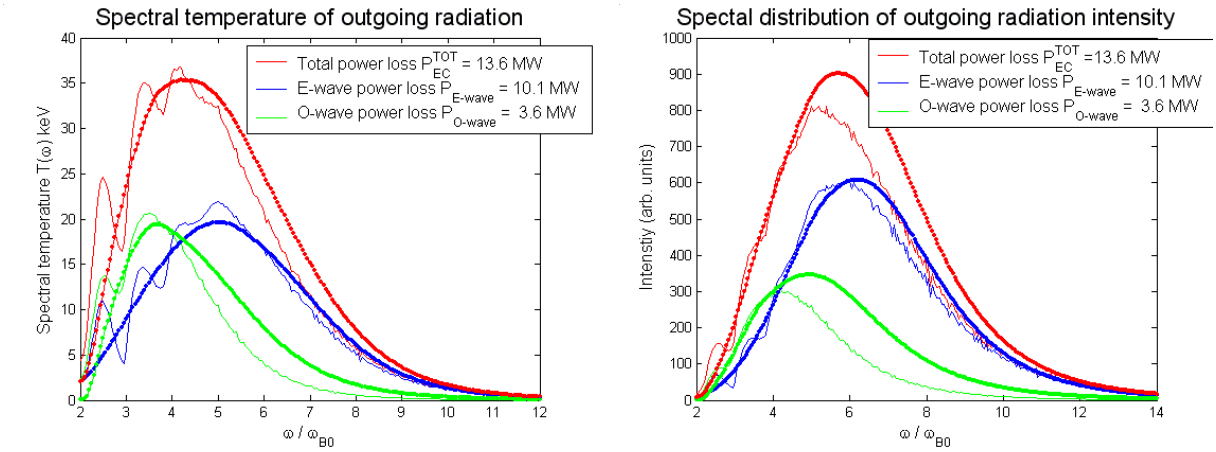

FIG. 2. Similar picture for the profiles of Eqs. 1,3.

Deviation of spectral temperature of EC radiation from local electron temperature determines the spectral density of the local ECR power loss in maxwellian plasmas. The remaining integration over frequency to evaluate the profile $P_{EC}(r)$ has to be done numerically:

$$P_{EC}(\rho) = 4\pi C \tau n_e(\rho) B_0^3 a^{-1} \sum_K \int_{\omega_{cut}(\rho)}^{\infty} \chi_K(\omega, T_e(\rho)) \omega^2 [T_e(\rho) - T_{ECR}(\omega, K)] d\omega \quad , \qquad (10)$$

where C = 3.9 10^{-8} MW/m^3 (B_0 and effective minor radius 'a' are in Tesla and meters).

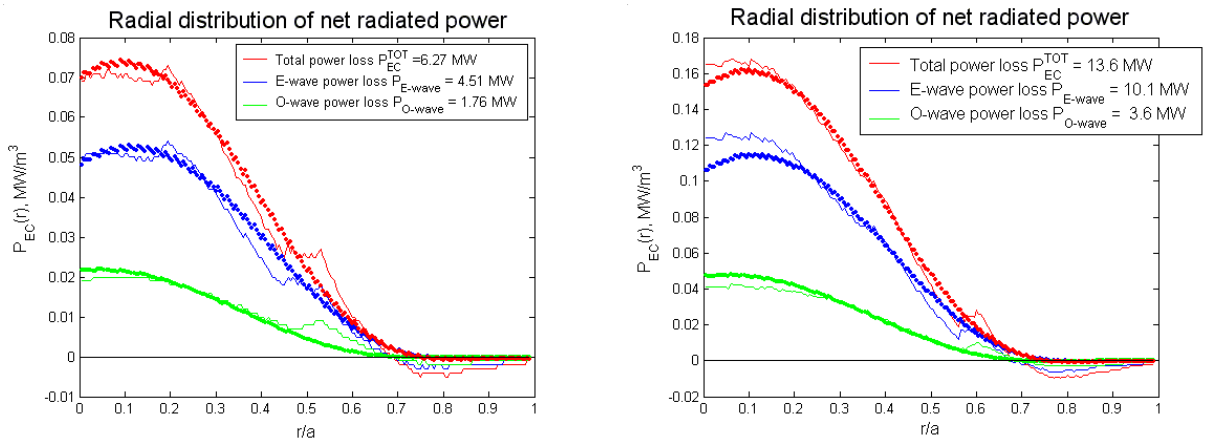

FIG. 3. Comparison of profiles $P_{EC}(r)$ of Eq. (10) (dots) with CYNEQ calculations (solid) for conditions of Figure 1 (left) and 2 (right).

3. **ECRH/ECCD-Produced Superthermal Electrons**

The deviation from a maxwellian was shown, with the help of the Fokker-Planck modeling of EDF, to be appreciable for high enough intensity of the injected waves [9]. Here we evaluate the formation of ECCD/ECRH-produced superthermal electrons with the help of the Fokker-Planck modeling of the EDF in parallel and perpendicular velocities on a given set of magnetic surfaces, via successive use of the numeric codes TORBEAM [3] and RELAX [4]. First, the beam tracing code TORBEAM calculates a power deposition profile and provides the beam width, *w*, and the variation of parallel refractive index, $\Delta N_{||}$, on the set of magnetic flux surfaces. Second, the fully relativistic Fokker-Planck code RELAX takes *w* and $\Delta N_{||}$ from TORBEAM and calculates, with allowance for resonance broadening [10], the EDF, power deposition and driven current. The steady-state EDF is obtained by iterations in time. Here we do not deal with the ITER geometry and perform a calculation for concentric circular flux surfaces with the proper dimensions R=6.2 m and a=2.0 m from ITER, for beams (O mode, n=1, total power 20 MW) launched in the equatorial plane to fit with use of the mid-plane launcher in ITER rather than the upper launcher. To test the maximal possible impact of injected wave on the EDF we analyze the case of wave beam focusing in the plasma core and full absorption of the injected power. It appears that under the above-mentioned conditions the EC absorbed power density may attain ~10 MW/m^3.

An analysis of EDFs calculated with the Fokker-Planck modeling is worth to carry out in the frames needed for evaluating the effect of superthermals on the $P_{EC}(r)$ profile with the code CYNEQ. The latter (see Sec. 4) requires EDF as a function of two variables: magnetic surface (or effective radial coordinate r) and electron energy E. This corresponds to averaging the EDF, calculated with TORBEAM + RELAX code, over magnetic surface and electron pitch angles. In principle, this pitch angle average will be a function of the bounce angle and thus not constant on the flux surface. Just to estimate the effect, we proceed by extracting only the deviation from a maxwellian with respect to electron energy and neglect any pitch angle dependence. The deviations of the resulted EDF, $f(E,r)$, from a maxwellian is most

appropriate to express in terms of an effective temperature, defined as EDF's exponential slope with respect to relativistic total electron energy E, namely

$$T_{eff}(E,r) \equiv -\left\{\partial \ln\left[f(E,r)\right]/\partial E\right\}^{-1}, \qquad (11)$$

The ratio of the effective temperature to that for the undisturbed maxwellian background, $T_{eff}(E,r)/T_e(r)$, indicated on the presence of superthermal fraction in the EDF when such a normalized effective temperature exceeds the unity.

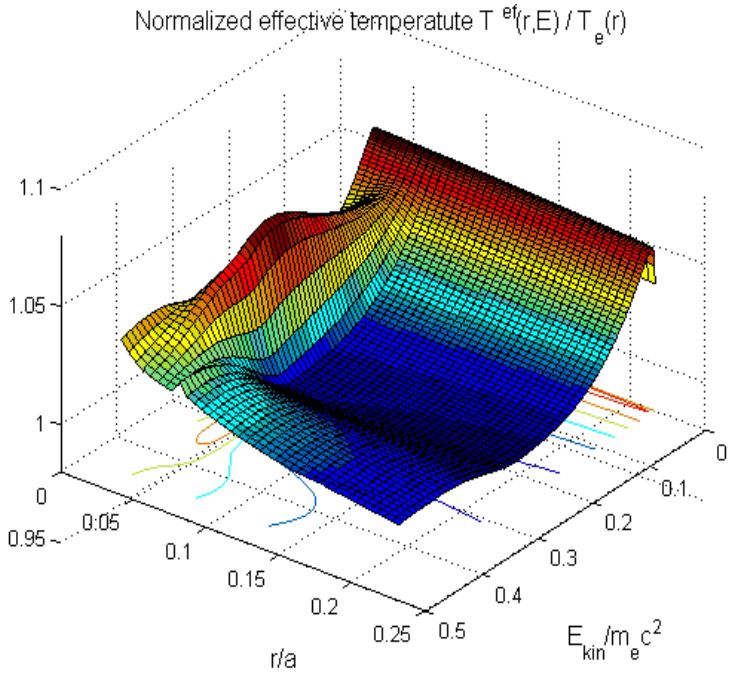

FIG. 4. The ratio $T_{eff}(E,r)/T_e(r)$ as a function of normalized radius and electron kinetic energy, for ECCD in the range r/a=(0,0.2) and oblique launch (toroidal injection angle β=22°, f=170 GHz), and $T_e(0)$ = 25 keV.

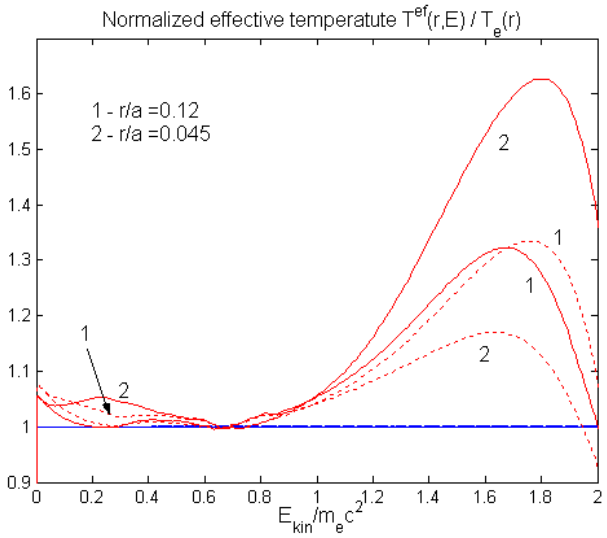

FIG. 5. The ratio $T_{eff}(E,r)/T_e(r)$ at two radii for the conditions of Figure 4 with $T_e(0)$ = 25 keV (solid) and 35 keV (dashed). The energy range of Figure 4 pertains to the left part of this figure (E_{kin}/m_ec^2 < 0.5). The peaks in the right part correspond to the plateau at electron momenta p/m_ec ~2.

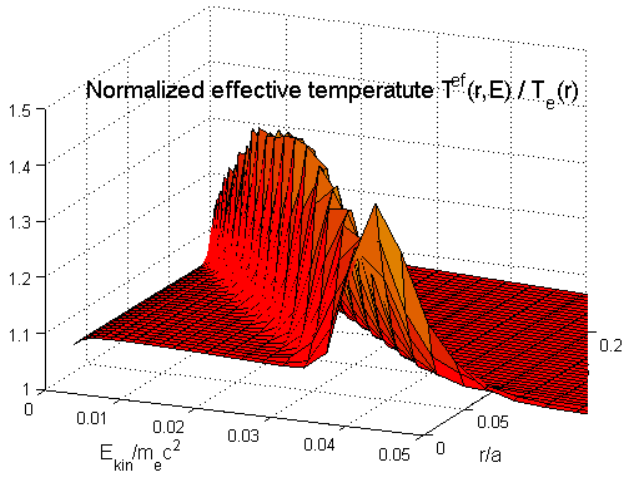

FIG. 6. The picture similar to Fig.4, for the case of ECRH (perpendicular launch, f=138 GHz) in the range r/a=(0,0.2), and $T_e(0)$ = 35 keV.

For perpendicular launch (ECRH only), the deviation of the EDF from the maxwellian is stronger for the thermal part ($E_{kin} < T_e$), with the effective temperature $T_{eff}(E_{kin})$ exceeding T_e by 10-20% and 20-40% for, respectively, $T_e(0)$ = 25 and 35 keV (Fig. 6). For oblique launch (ECCD/ECRH), with an injection angle $\beta \sim 20°$, T_{eff}/T_e is about twice smaller, but in a substantially broader energy range, up to $E_{kin}/m_e c^2 \sim 0.5$, producing thus a strong enough fraction of superthermal electrons (Figs. 4,5). Also, formation of a plateau on the EDF at higher energies is found ($E_{kin}/m_e c^2 \sim 1$, $T_{eff}/T_e \sim 2$-5) for both launch geometries (cf. Fig. 5).

4. ECR Power Loss Density Profile Under ECCD/ECRH

The results of evaluating, with the code CYNEQ, the effect of superthermals on the $P_{EC}(r)$ profile show how the distortions of the EDF caused by the absorption of external intense ECR, injected into the plasma at low harmonics of the cyclotron frequency (n=1) for ECRH and ECCD, influence the transport of ECR, emitted by the plasma itself at all other harmonics (2<n<15) responsible for formation of the $P_{EC}(r)$ profile in reactor-grade tokamaks. For the conditions, close to inductive (Eqs. (1),(2)) and steady-state ITER regimes (Eqs. (1),(3)), we found the following dependence of $P_{EC}(r)$ on the geometry of ECRH/ECCD, for a 20 MW beam with beam focusing in the core and full absorption in the plasma.

For perpendicular launch, the relative change of the profile $P_{EC}(r)$ is small (~ few percents in the core for $T_e(0)$ = 25 keV, see Fig. 8). For oblique launch the largest relative rise of $P_{EC}(r)$ in the core attains 10~20% (for injection angle $\beta \sim 20°$, Fig. 7), because in this case the EC power is absorbed by electrons with larger velocity (and, respectively, smaller rate of relaxation to a maxwellian due to the pair Coulomb collisions). If the calculated steady-state ECRH/ECCD-disturbed EDF is violently converted to a maxwellian with the same relativistic mean electron energy, we obtain similar or slightly larger effect on the $P_{EC}(r)$ profile.

The value of the effect for perpendicular launch appears to be similar to that in the case [2(B,C)], when EDF's distortions are caused exclusively by the ECR emitted by the plasma (total power of this ECR inside the tokamak chamber may be estimated as P_{EC}^{tot} $[1+R_w]/[1-R_w]$ that amounts to ~20 MW in ITER scenario 2 with wall reflection coefficient R_w=0.6).

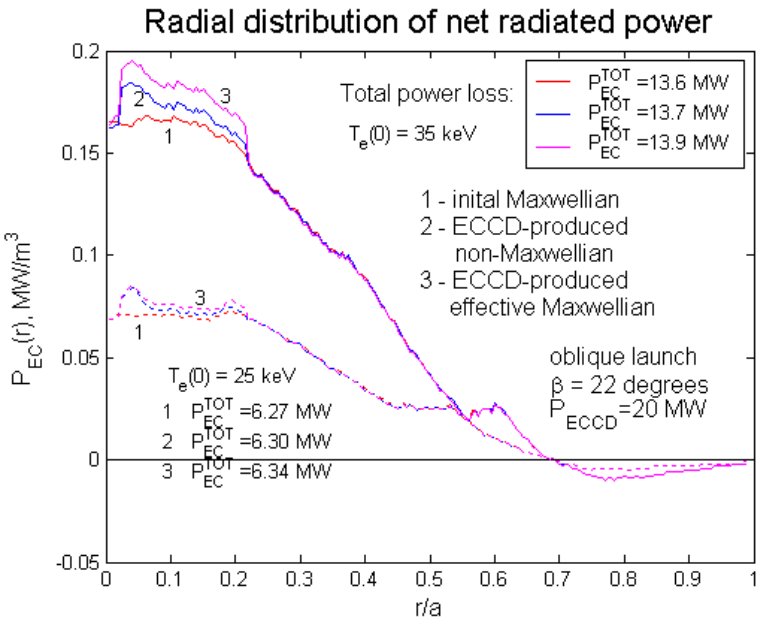

FIG. 7. Comparison of radial profiles of net ECR power loss for maxwellian background plasma (curve 1), non-maxwellian EDF under the condition of ECCD of 20 MW total power with beam focusing in the center (n=1, O-mode, f=170 GHz, oblique launch in equatorial plane with toroidal injection angle β=22°) (curve 2), and maxwellian EDF with the same relativistic mean electron energy (curve 3), for wall reflection coefficient R_W=0.6.

Relative change of radial profiles both for oblique launch, f=170 GHz (Fig.7) and perpendicular launch, f=138 GHz, are shown in Figure 8.

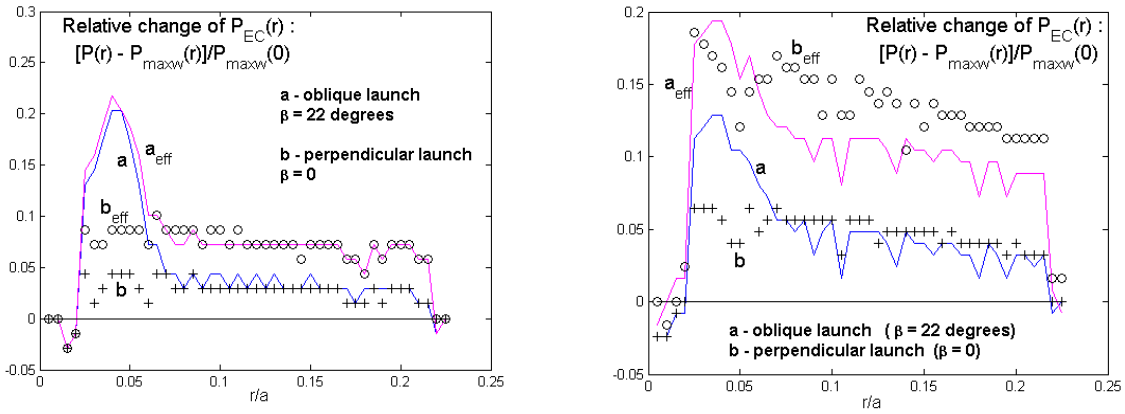

FIG. 8. Relative change of radial profiles in the region of ECCD/ECRH (r/a < ~0.2) for oblique (solid curve, a) and perpendicular (crosses, b) launch vs. profile for background maxwellian with $T_e(0)$ = 25 keV (left) and $T_e(0)$ = 35 keV (right). Similar comparison of the effective maxwellian (i.e. maxwellian EDF with the same relativistic mean electron energy) is given by the solid curve (a_{eff}) and the circles (b_{eff}).

5. Conclusions

a) Analysis of comparing the CYNEQ and CYTRAN calculation procedures enables us to simplify further the fast routine of CYTRAN and retain reasonable accuracy of describing the radial profile of EC net radiated power, $P_{EC}(r)$, in the region of significant contribution of $P_{EC}(r)$ to the local power balance in fusion reactor-grade tokamaks (first

of all, in the central part of the plasma column). The resulted analytic description is to be used as a simple simulator during the transport calculations for fusion reactor-grade tokamaks.

b) The effect of ECCD/ECRH-produced superthermal electrons on the net ECR power loss density, $P_{EC}(r)$, for the same value of total absorbed EC power is stronger for power absorption at larger electron velocities. For equatorial plane launch, the effect is maximal (~ 20 %) for wave beam focusing in the core and toroidal injection angle ~ 20°.

c) At present the ECCD is calculated with ignoring the contribution of ECR harmonics higher than that of the injected wave because the ECCD wave spectral intensity is much higher than that for plasma's ECR. However, in ITER the total power of 20 MW ECCD wave will be comparable to that of plasma's ECR inside the chamber (e.g., ~ 20 MW for scenario 2 with R_w=0.6). As far as the ECCD is resulted exclusively from the asymmetry of the electron velocity distribution function in the co- and counter-current directions, the impact of plasma's ECR on the ECCD may not be small and has to be evaluated.

Acknowledgments

The present work is partly supported by the NOW-RFBR Grant Nr.047.016.016, the Russian Federal Agency on Science and Innovations (contract 02.445.11.7505), and the Atomic Science and Technology Department of Russian Federal Atomic Energy Agency. Participation of A.B.K. in the 21st IAEA Fusion Energy Conference is supported by the travel grant from the IAEA.

References

[1] ALBAJAR, F., BORNATICI, M., CORTES, G., et al., Nucl. Fusion, **45** (2005) 642; Proc. 31st Eur. Phys. Soc. Conf. Plasma Phys. and Contr. Fusion (London, U.K., 2004), ECA Vol. 28G, P-4.171 (http://epsppd.epfl.ch/London/pdf/P4_171.pdf).

[2] CHEREPANOV, K.V., KUKUSHKIN, A.B., (A) Proc. 20th IAEA Fusion Energy Conference. (Vilamoura, Portugal, 2004), TH/P6-56; (B) Proc. 31st Eur. Phys. Soc. Conf. Plasma Phys. and Contr. Fusion (London, U.K., 2004), ECA vol. 28, P-1.175. http://epsppd.epfl.ch/London/pdf/P1_175.pdf; (C) Proc. 32nd Eur. Phys. Soc. conf. on Plasma Phys. and Contr. Fusion (Tarragona, Spain, 2005), ECA, vol. 29C, P-2.117 (http://epsppd.epfl.ch/Tarragona/pdf/P2_117.pdf).

[3] POLI, E., et al., Comp. Phys. Commun., **136** (2001) 90.

[4] WESTERHOF, E., PEETERS, A.G., SCHIPPERS, W.L., Rijnhuizen Report RR 92-211 (1992).

[5] POLEVOI, A.R., MEDVEDEV, S.YU., MUKHOVATOV, S.V., et al., J Plasma Fusion Res. SERIES, **5** (2002) 82-87.

[6] TAMOR, S., (A) Fusion Technol., **3** (1983) 293; Nucl. Instr. and Meth. Phys. Res., **A271** (1988) 37; (B) Reps. SAI-023-81-110-LJ/ LAPS-72 and SAI-023-81-189-LJ/ LAPS-72, La Jolla, CA: Science Applications (1981).

[7] KUKUSHKIN, A.B., (A) Proc. 14th IAEA Conf. on Plasma Phys. & Contr. Fusion, Wuerzburg, 1992, v. 2, p. 35-45; (B) Proc. 24th EPS Conf. on Contr. Fusion & Plasma Phys., Berchtesgaden, 1997, ECA vol. 21A, Part II, p. 849-852**.**.

[8] ALBAJAR, F., BORNATICI, M., ENGELMANN, F., Nucl. Fusion, **42** (2002) 670.

[9] HARVEY, R.W., et al., Phys. Rev. Lett., **62** (1989) 426.

[10] WESTERHOF, E., Proc. 9th Joint Workshop ECE & ECH, 1995, p. 3.